Niche Partitioning Between Coastal and Offshore Shelf Waters Results in Differential Expression of Alkane and PAH Catabolic Pathways

Shawn M. Doyle[a#], Genmei Lin[b], Maya Morales-McDevitt[c], Terry L. Wade[a,d], Antonietta Quigg[a,e], and Jason B. Sylvan[a#]

[a]Department of Oceanography, Texas A&M University, College Station, TX, USA.
[b]School of Marine Sciences, Sun Yet-Sen University, Zhuhai, China.
[c]Graduate School of Oceanography, University of Rhode Island, Narragansett, RI, USA.
[d]Geochemical and Environmental Research Group, Texas A&M University, College Station, TX, USA
[e]Department of Marine Biology, Texas A&M University at Galveston, Galveston, TX, USA.

Running title: **Niche partitioning of oil degrading bacterial ecotypes**

Abstract word count: 232 for abstract, 120 for importance
Main text word count: 4998

[#]Corresponding authors:
Shawn M. Doyle
Jason B, Sylvan
Department of Oceanography
Texas A&M University
Eller O&M Bldg, Rm 716
College Station, TX, 77843-3146
Tel: 979-845-5105
E-mail: shawndoyle@tamu.edu
jasonsylvan@tamu.ediu

ABSTRACT

Marine oil spills can impact both coastal and offshore marine environments, but little information is available on how the microbial response to oil and dispersants might differ between these biomes. Here we describe the compositional and functional response of microbial communities to different concentrations of oil and chemically dispersed oil in coastal and offshore surface waters from the Texas-Louisiana continental shelf. Using a combination of analytical chemistry, 16S rRNA amplicon, and metatranscriptomic sequencing, we provide a broad, comparative overview of the specific functional and ecological response of hydrocarbon degrading bacteria in marine surface waters over time between two oceanic biomes. We found evidence for the existence of different ecotypes of several commonly described hydrocarbon degrading bacterial taxa which behaved differentially in coastal and offshore shelf waters despite being exposed to similar concentrations of oil, dispersants, and nutrients. This resulted in the differential expression of catabolic pathways for n-alkanes and polycyclic aromatic hydrocarbons (PAH)—the two major categories of compounds found in crude oil—with preferential expression of n-alkane degradation genes in coastal waters while offshore microbial communities trended more towards the expression of PAH degradation genes. This was unexpected as it contrasts with the generally held view that n-alkanes, being more labile, are attacked before the more refractory PAHs. Collectively, our results provide new insights into the existence and potential consequences of niche partitioning of hydrocarbon degrading taxa between neighboring marine environments.

IMPORTANCE

In the wake of the Deepwater Horizon oil spill, the taxonomic response of marine microbial communities to oil and dispersants has been extensively studied. However, relatively few studies on the functional response of these microbial communities have been reported, especially in a longitudinal fashion. Moreover, despite the fact that marine oil spills typically impact thousands of square kilometers of both coastal and offshore marine environments, little information is available on how the microbial response to oil and dispersants might differ between these biomes. The results of this study help fill this critical knowledge gap and provide valuable insight into how oil spill response efforts, such as chemically dispersing oil, may have differing effects in neighboring coastal and offshore marine environments.

90 **INTRODUCTION**

91 Crude oils are complex mixtures of thousands of different compounds, ranging from
92 saturated alkanes and aromatic hydrocarbons to complex, heteroatom-containing resins
93 and asphaltenes (1). While some of these compounds are recalcitrant to degradation, many
94 can be utilized as a carbon or energy source by microorganisms (2). Microbial
95 biodegradation is one of the primary means by which both natural and anthropogenic oil
96 releases are bioremediated in nature. However, many crude oil hydrocarbons are poorly
97 soluble, which lowers their availability to microorganisms and limits biodegradation rates.
98 As such, chemical dispersants have been used after marine oil spills to disperse oil into the
99 water column with the aim of dramatically increasing the surface area for microbial attack
100 (3). Despite this, studies have reported conflicting results on whether chemical dispersants
101 improve or suppress oil biodegradation rates by microbes (4–8).

102 The Deepwater Horizon (DwH) oil spill involved the release of ~780,000 m^3 crude
103 oil into the Gulf of Mexico after which 7000 m^3 chemical dispersants were used during the
104 spill response effort (9, 10). The magnitude of the spill led to a surge of research into the
105 microbial ecology of marine oil spills and dispersant usage both in deep-sea habitats (11–
106 15) and shoreline environments such as beaches (16–19) and salt marshes (20, 21).
107 However, much less information is available on the responses of microbial communities in
108 surface waters on the continental shelf (22). These areas in the Gulf of Mexico range from
109 river-dominated, nutrient rich waters along the coasts to near oligotrophic waters on the
110 continental shelf edge. Oil spills can affect many thousands of square kilometers of both
111 open ocean and coastal habitats, and the microbial communities which inhabit these
112 respective marine biomes can differ substantially in composition, structure, and metabolic

113 potential (23, 24). As a result, natural biodegradation of oil spills likely varies considerably
114 across different shelf water regimes. Understanding how microbial communities inhabiting
115 these different ocean biomes respond to oil and dispersants consequently represents an
116 important research need.

117 To better define the ecological and functional response of marine microorganisms to
118 oil, we conducted mesocosm experiments using coastal seawater collected from the
119 continental shelf (herein referred to as Coastal) and offshore waters on the edge of the
120 shelf (herein referred to as Offshore) of the northwestern Gulf of Mexico (Figure S1, Table
121 S1) and amended them with oil or chemically dispersed oil. The responses of the microbial
122 communities were subsequently followed over time using cell counts, 16S rRNA amplicon
123 and metatranscriptomic sequencing. This analysis allowed us to identify which groups of
124 bacteria responded to oil with and without dispersant and also characterize the functional
125 response of hydrocarbon-degrading microbes within the communities. Our results
126 revealed that ecotype differences between coastal and offshore communities resulted in
127 differential expression of alkane and PAH catabolic pathways between these oceanic
128 biomes and that the response to dispersants was variable by location.

129 **RESULTS**

130 **Hydrocarbon Chemistry**

131 We tracked total alkane and PAH concentrations over time using a combination of
132 GC/FID and GC/MS, respectively (Figure 1, Table S2). In the Control treatments of both
133 experiments, these concentrations were <5 μg L^{-1} for both classes of compounds with one
134 exception: the seawater used in the Coastal experiment naturally contained a low
135 concentration, roughly 20 μg L^{-1}, of n-alkanes. In the WAF treatments of both experiments,

136 alkane concentrations were also very low and did not differ substantially from those
137 observed in the Controls while initial PAH concentrations were elevated to ~50 μg L^{-1}. In
138 the DCEWAF and CEWAF treatments, chemically dispersing the oil increased initial alkane
139 concentrations to ~325 μg L^{-1} and ~3000 μg L^{-1}, respectively. Initial PAH concentrations
140 within these two dispersed oil treatments were also increased, but more modestly, to ~100
141 μg L^{-1} and ~400 μg L^{-1}, respectively.

142 **Microbial cell abundance**

143 Average cell abundances (Figure S2) were typical for seawater, ~10^6 cells mL^{-1} (25,
144 26). The average abundance in the Coastal experiment (2.4±0.7 ×10^6 cells mL^{-1}) was
145 twofold that in the Offshore experiment (1.3±0.5 ×10^6 cells mL^{-1}). Between treatments, cell
146 abundances were ~1.7-fold higher in the Coastal CEWAF treatment [$F(3,20)=11.5$,
147 $p<0.001$] than in the Control, WAF, and DCEWAF treatments, where cell abundances were
148 similar [$F(2,18)=1.22$, $p=0.32$]. In the Offshore experiment, cell abundances were instead
149 slightly lower (1.6-fold) in the Control treatment [$F(3,32)=3.03$, $p=0.04$], while those in the
150 WAF, DCEWAF, and CEWAF remained similar [$F(2,24)=0.78$, $p=0.47$]. Though the overall
151 effect was relatively small, we did observe slight increases in cell abundance over time in
152 both experiments within the two treatments containing the most oil (i.e. DCEWAF and
153 CEWAF) while those in the Control and WAF began to decrease towards the end of each
154 experiment.

155 **Microbial community composition**

156 We profiled the composition and structure of the microbial communities using 16S
157 rRNA amplicon sequencing (Figure 2). NMDS ordination of Bray-Curtis dissimilarities (BC-
158 D) revealed that in the Offshore experiment, samples formed four distinct clusters

159 organized sequentially by the four treatments (Figure S3A and S3E). Relative to the Control
160 treatments, communities exposed to WAF were the most similar (BC-D: 0.30 ± 0.09; avg ±
161 SD), followed by DCEWAF (0.47 ± 0.13), and finally CEWAF (0.59 ± 0.14). A similar pattern
162 was observed in the Coastal experiment. Communities exposed to CEWAF were the most
163 distinct from the Controls (0.82 ± 0.10), followed by the DCEWAF (0.58 ± 0.14) and WAF
164 (0.39 ± 0.09), respectively.

165 In total, we detected 2880 ASVs across both experiments. Compositionally,
166 *Gammaproteobacteria* was the most abundant group observed, constituting an average of
167 77.4% and 67.0% of the overall communities within the Offshore and Coastal experiments,
168 respectively (Figure 2, Figure S4). Within this class, dominant taxa included
169 *Alteromonadales* (*Alteromonas*, *Marinobacter*, and *Aestuariibacter*), *Thiotrichales*
170 (*Methylophaga* and *Cycloclasticus*), *Oceanospirillales* (*Alcanivorax*, *Oleibacter*, and
171 *Thalassolituus*), and *Xanthomonadales* (*Polycyclovorans*) (Figure S5).

172 **Identification of oil-enriched ecotypes**

173 ASVs from the same genus often varied in how they responded to oil or dispersed oil
174 (Table S5). These differences occurred both between treatments and between the two
175 experiments. In order to more accurately define potential ecotype responses, we used
176 redundancy analysis (RDA) modeling to narrow our dataset and identify only those ASVs
177 which were directly enriched by oil within the WAF, DCEWAF, and CEWAF treatments. In
178 each model, variables for both time and initial oil concentration contributed significantly
179 (p<0.001) to the RDA models (Figure S3, B-D and F-H). Using scalar projections of ASVs
180 onto the *Oil* vector in each model, we identified 30 oil-enriched ASVs between the two

181 experiments, 8 of which were identified in both the offshore and coastal shelf water
182 mesocosms (Figure 3).
183 The response of many oil-enriched ASVs to each treatment was notably different
184 between the two experiments. For example, we found three *Alcanivorax*-related ASVs were
185 enriched by oil in the Coastal experiment, but in the Offshore experiment these were either
186 very rare (e.g. ASV33 and ASV36) or were not significantly more abundant in the oil
187 amended treatments versus the Control (ASV16). Likewise, ASV8 (*Polycyclovorans*)—an
188 obligate hydrocarbon degrading taxa which inhabits the phycosphere of marine diatoms
189 and dinoflagellates (27)—was present in both experiments, but was enriched by oil in only
190 the Offshore experiment. We also found several ASVs belonging to the same genera which
191 exhibited differential responses to oil between the two experiments. For example, ASV2
192 (*Marinobacter*) was highly abundant in the Coastal treatments (11.9%; average relative
193 abundance), but was comparatively sparse Offshore (0.3%). Meanwhile, another
194 *Marinobacter*-related ASV (ASV19), was abundant in the Offshore WAF, DCEWAF, and
195 CEWAF treatments, but was restricted to only the WAF treatment in the Coastal
196 experiment. Lastly, ASV11 (*Cycloclasticus*) increased in relative abundance over time in all
197 three oil-amended Offshore treatments, but was unexpectedly nearly absent in the Coastal
198 CEWAF.
199 **Identification of hydrocarbon degradation gene transcripts**
200 We parsed the metatranscriptome datasets to identify and quantify the expression
201 of hydrocarbon degradation gene transcripts within the mesocosms. A GHOSTX query of
202 the KEGG database identified 6195 transcripts affiliated with hydrocarbon degradation
203 genes. An additional 163 transcripts were identified as alkane hydroxylating P450 genes

204 from the CYP153 family through a custom BLASTP search. We compared the abundance of
205 these hydrocarbon degradation gene transcripts between each oil-amended treatment and
206 its respective control treatment and used an outlier analysis to estimate the number of
207 upregulated genes at each time point (Figures S6 and S7). Within both experiments, this
208 number was generally higher in the DCEWAF and CEWAF treatments versus the WAF
209 treatments. We also observed that the number of upregulated genes increased overtime in
210 dispersant-amended treatments, but decreased overtime in WAF.

211 We next sought to test if the amount of upregulation among these upregulated
212 hydrocarbon degradation genes was affected by treatment. Highly expressed hydrocarbon
213 degradation gene transcripts were on average 10.4-fold more abundant in the oil-amended
214 treatments than in the Controls. However, using a factorial ANOVA test with pairwise
215 comparisons of the oil-amended treatments, we found only minor significant differences
216 between treatments (0.1 to 1.2-fold). In other words, the expression of upregulated
217 hydrocarbon degradation genes was higher in the WAF, DCEWAF, and CEWAF treatments
218 over the Controls, but by about the same amount per oil-amended treatment (Figure S8).
219 This indicates that the expression of hydrocarbon degradation genes was primarily
220 structured by microbial community turnover—which we observed in our 16S rRNA
221 amplicon dataset—rather than changes gene expression among community members.

222 **Coastal versus offshore expression of n-alkane and PAH degradation pathways**

223 To compare differences in the expression of hydrocarbon catabolic pathways in our
224 experiments, we consolidated the identified gene transcripts into four metabolic
225 categories: [1] n-alkane activation, [2] beta-oxidation of fatty acids, [3] ring-
226 hydroxylating/cleaving dioxygenases, and [4] PAH degradation (Figure 4). Alkane

227 degradation begins with terminal oxidation of the substrate to a primary alcohol with a
228 hydroxylase or monoxygenase enzyme (e.g. AlkB). The resulting alcohol is further oxidized
229 to a fatty acid by alcohol and aldehyde dehydrogenases before entering the beta oxidation
230 pathway (28). Likewise, PAH degradation typically begins with ring hydroxylation and
231 subsequent cleavage with dioxygenase enzymes (29), the products of which are then
232 channeled through various complex, multi-step catabolic pathways (30). Hence, these four
233 categories together represent the activation [1+3] and subsequent degradation [2+4]
234 pathways for saturated hydrocarbons (i.e. linear and cyclo- alkanes) and PAHs,
235 respectively, to central metabolism intermediates.

236 Alkane activation gene transcripts were observed primarily in the DCEWAF and
237 CEWAF treatments of the Coastal experiment where they were produced almost entirely by
238 *Marinobacter* and *Alcanivorax* (Figure 4). In comparison, expression of alkane degradation
239 genes in the Coastal WAF and Control treatments was very low (~28 TPM; transcripts per
240 million transcripts). This was consistent with the very low total alkane concentrations we
241 measured in these two treatments (< 14 ug/L; Figure 1). In the Offshore experiment,
242 expression of genes involved with alkane activation was instead comparatively low across
243 all four treatments.

244 Expression of fatty acid beta-oxidation genes was the highest of the four metabolic
245 categories, reflecting the nearly universal taxonomic distribution of this pathway [69]. In
246 the Coastal experiment, highest expression levels were again observed in the DCEWAF and
247 CEWAF with comparatively lower expression levels in the WAF and Control treatments.
248 Similar to the alkane activation genes, fatty acid beta-oxidation genes in the Coastal
249 experiment were expressed in large part by *Marinobacter* and *Alcanivorax* (Figure 4).

250 However, significant expression of *Alteromonas*, *Aestuariibacter*, *Oleibacter*, and
251 *Pseudomonas*-assigned transcripts were observed in this category as well. In the Offshore
252 experiment, abundant transcripts were detected from *Alteromonas* in all four treatments,
253 while those from *Marinobacter, Aestuaribacter* and *Alcanivorax* were mainly observed in
254 DCEWAF and CEWAF.

255 In contrast to the alkane degradation categories, overall expression for ring
256 cleavage/hydroxylation dioxygenase and PAH degradation genes was significantly higher
257 in the Offshore experiment (Figure 5). *Cycloclasticus*, a genus of obligate PAH degraders
258 (31), were the primary source of detected ring cleavage/hydroxylation dioxygenase gene
259 transcripts (~27% of all transcripts in these two categories) across both experiments.
260 These *Cycloclasticus*-derived dioxygenase gene transcripts were observed in every sample
261 except the Controls and the Coastal CEWAF. This pattern was also observed in our 16S
262 rRNA amplicon dataset wherein the relative abundance patterns of ASV11 (*Cycloclasticus*)
263 was substantially lower in the Coastal CEWAF treatments (Figure 3). Other taxa to which a
264 significant portion of dioxygenase and PAH degradation gene transcripts were assigned to
265 were *Halomonas*, *Halioxenophilus*, unclassified *Gammaproteobacteria*, and unclassified
266 Bacteria (Figure 4).

267 In both experiments, there was a general decrease with increasing oil
268 concentrations in the alpha diversity of expressed genes involved in alkane degradation
269 (CEWAF > DCEWAF > WAF > Control) (Figure 6). However, this effect disappeared in the
270 categories for PAH degradation, where instead a large drop in alpha diversity occurred for
271 all treatments with added oil, but the difference between the three oil-amended treatments
272 was minimal.

273 **DISCUSSION**

274 In this study, we found initial oil concentration strongly structured the microbial
275 communities. Many of the identified bacteria belong to hydrocarbon degrading taxa which
276 are known to bloom in seawater during oil spills or near natural oil seeps (2, 32, 33).
277 However, we also found evidence that many of these taxa were composed of ecotypes
278 which responded remarkably different to oil and dispersants in coastal and offshore shelf
279 waters. These differences were reflected in the expression of hydrocarbon degrading
280 genes, resulting in unexpected differences in alkane and PAH degradation pathways
281 between the two oceanographic zones. Interestingly, patterns in the diversity of expressed
282 hydrocarbon genes did not vary substantially between environments, indicating that some
283 aspects of the response of microbial communities in marine surface waters to oil or
284 chemically dispersed oil exposure may be common between locales. Overall, these findings
285 highlight that natural remediation processes such as microbial biodegradation are not
286 uniform across different ocean biomes and reinforce the need for a better understanding of
287 the spatial and temporal variances in natural oil remediation processes.

288 **Ecotype Dynamics**

289 Following the distinct clustering we observed in the NMDS ordinations, many of the
290 oil-enriched taxa (e.g. *Marinobacter*, *Alteromonas*, *Alacnivorax*, and *Polycyclovorans*)
291 appeared to bloom in response to increasing oil concentrations, while others (e.g.
292 *Methylophaga*) appeared to primarily be either inhibited or outcompeted by organisms
293 increasing in relative abundance. *Alteromonas* and *Aestuaribacter* were identified as oil-
294 enriched in our 16S rRNA dataset (Figure 3) and have been repeatedly identified in
295 laboratory and field based 16S rRNA surveys of marine oil spills (2, 34–37). In our

296 metatranscriptomes, these two taxa were almost exclusively responsible for expression of
297 fatty acid oxidation genes. This suggests that these two taxa were primarily secondary
298 alkane degraders relying on other community members to activate alkanes (38).
299 *Halomonas* were detected in the CEWAF treatments, but were not abundant elsewhere. It
300 was not one of the ASVs enriched by oil, and is not known for PAH degradation, so it may
301 also have responded to secondary metabolites in the CEWAF treatments.
302 *Halioxenophilus* are known to degrade xylene (39), but this newly discovered genus
303 has not been reported to degrade PAHs in an environmental context previously. In our
304 study, PAH degradation gene transcripts assigned to *Halioxenophilius* indeed belonged to
305 the xylene degradation pathway (Figure 5) and were detected in equal abundance in both
306 the Coastal and Offshore experiments. However, the total abundance of this pathway was
307 substantially lower than the benzoate degradation pathway, indicating this genus likely
308 catalyzes a secondary "shunt" for PAH degradation intermediates.
309 **Differential Expression of Alkane and PAH Catabolic Pathways**
310 Several factors are at play when considering the ecological dynamics of alkane and
311 PAH degrading microorganisms in marine environments. First is the relative metabolic
312 complexity of these two processes. The catabolic pathway for alkane degradation is
313 comparatively simple: the activation of an alkane to a fatty alcohol is a single step process
314 through the action of an alkane hydroxylase (40). Once an alkane is activated, the
315 subsequent fatty alcohol quickly feeds through a couple intermediates into the beta-
316 oxidation pathway to produce several acetyl-CoA molecules, a central TCA cycle
317 intermediate. In contrast, PAH degradation involves a complex series of multi-enzyme ring
318 hydroxylation and ring cleavage steps (30). Considering the energetic costs with

319 synthesizing these enzymes, there is likely a fitness cost associated with biodegrading
320 PAHs, especially those of high-molecular weight, compared to biodegrading alkanes. This is
321 consistent with patterns of crude oil weathering typically observed in the environment,
322 where the alkane fraction of crude oil typically disappears faster than the PAH fraction
323 (41–44).

324 One of the most striking results from our metatranscriptomic datasets was the
325 difference in the expression of alkane and PAH catabolic pathways between the Coastal and
326 Offshore experiments. In particular, the substantially lower expression of alkane activation
327 genes concurrently with increased expression of PAH degradation genes in the Offshore
328 experiment (Figure 5) was unexpected as it contrasts with the above notion that n-alkanes
329 are more labile and are attacked before the more refractory PAHs. This is not due to a lack
330 of alkane degrading taxa—known alkane degrading species such as *Marinobacter* (45),
331 *Thalassolituus* (46), and *Oleibacter* (47) were present in both experiments (Figure 3).

332 Laboratory studies have estimated that the input of phytoplankton-derived alkane
333 production into marine surface waters is ~100-fold greater than the combined inputs from
334 oil spills and natural oil seeps (48) and can sustain populations of alkane-degrading
335 bacteria which rapidly expand upon exposure to crude oil (49, 50). Thus, the differences in
336 alkane activation transcripts we observed between the two experiments may be due to a
337 priming effect from the larger abundances of phytoplankton typically observed in Gulf of
338 Mexico coastal shelf waters. Three lines of evidence in our data support this hypothesis: [1]
339 ASVs classified as Cyanobacteria and/or Chloroplasts were substantially more abundant in
340 our Coastal mesocosms than our Offshore mesocosms (Figure 2), [2] transcripts for
341 aldehyde-deformylating oxygenase—the key enzyme in cyanobacterial alkane biosynthesis

342 (51, 52)—were exclusively observed in our coastal metatranscriptomes, and [3] the
343 concentration of naturally present alkanes (i.e. in the Controls) was approximately 10-fold
344 higher in our coastal seawater samples than those collected offshore (Figure 1, Table S2).
345 With regards to the expression of PAH degradation pathways in our
346 metatranscriptomes, a major difference between the Coastal and Offshore experiment
347 appeared to be due to a differential response of *Cycloclasticus* ecotypes. Our data initially
348 appears to suggest that members of this genus are sensitive to highly concentrated
349 (~50ppm) CEWAF preparations. We have seen this before in a previous mesocosm
350 experiment we conducted with near-shore seawater: *Cyloclasticus*-related OTUs were
351 nearly completely absent in CEWAF treatments, but thrived in WAF and DCEWAF (34).
352 However, in the current study, this sensitivity enigmatically did not occur in the Offshore
353 experiment at all. In fact, in our metatranscriptomes, the Offshore CEWAF treatment
354 contained the largest abundance of *Cycloclasticus* affiliated dioxygenase and PAH
355 degradation gene transcripts. Furthermore, in our 16S rRNA datasets, *Cycloclasticus* related
356 ASVs were absent in the Coastal CEWAF but bloomed from 0.05% to 10.3% relative
357 abundance in the Offshore CEWAF (Figure 3). Although there is evidence that some
358 *Cycloclasticus* species are sensitive to high concentrations of inorganic nutrients (53) or
359 differences in temperature (54), this does not provide a valid explanation for our findings
360 as we amended all mesocosms with f/20 media and both experiments were performed at
361 the same temperature. Taken together, these new findings indicate that a strong selective
362 pressure against *Cycloclasticus* sp. occurred in coastal seawater at high concentrations of
363 chemically dispersed oil, but this negative selection was not solely due to nutrient
364 concentrations, the presence of chemical dispersants, or high concentrations of oil. Further

research will be needed to elucidate the cause of this apparent niche partitioning by *Cycloclasticus* ecotypes. Possibilities include variable physiological responses to oil exposure under different environmental regimes, or ecological competition with other microorganisms.

CONCLUSIONS

In this study, we showed that prokaryotic communities can respond in different ways to oil spills depending on the location of the spill, which is tightly tied to the starting initial community. In our experimental design, season, oil, dispersant, and inorganic nutrients were controlled for between the two experiments. Only community composition and potentially chemical characteristics not measured here were different, indicating that these were responsible for the different responses observed. This is important because oil spills can and do spread out over multiple marine realms (e.g. 2010 Deepwater Horizon, 1979 Ixtoc-1, Gulf War, and 1978 Amoco Cadiz oil spills). The response of microbial communities within those realms may vary and this should weigh into management and mitigation decisions during and after an oil spill. As was shown here, even within the same genus, different ecotypes may respond differently to oil and/or dispersant. Gene expression can vary on the community level between different environments facing the same spill. Previous work has shown that niche partitioning may be important to compositional responses to oil spills (7, 34), but this work is the among the first to show that gene expression is also impacted. We conclude that niche partitioning and ecotype dynamics play a critically important role in how marine environments response to past and future oil spills.

388 # MATERIALS AND METHODS

389 ## Mesocosm Experiments and Sampling

390 Surface seawater (1m) for the Coastal and Offshore mesocosm experiments were
391 collected at 29°38' N, 93°50' W, on July 16th, 2016 and at 29°53' N, 94°20' W, on July 9th,
392 2016, respectively (Figure S1, Table S1). The seawater was transferred to a holding tank in
393 the Texas A&M University at Galveston Sea Life Facility, covered, and stored at room
394 temperature overnight prior to experiment initiation. Four treatments were prepared in
395 triplicate as described previously in Doyle et al. (34): [1] "Control", containing only
396 seawater, [2] "WAF", containing seawater and oil supplied as a water-accommodated
397 fraction, [3] "CEWAF", containing seawater, oil, and Corexit supplied as a chemically-
398 enhanced water-accommodated fraction in a dispersant to oil ratio of 1:20, and [4]
399 "DCEWAF", a 1:10 dilution of the "CEWAF" treatment. The WAF and CEWAF was prepared
400 by adding 25 mL (5 mL every 30 min for 2.5 h) of Macondo surrogate oil (WAF) or oil plus
401 dispersant (CEWAF) into 130L of seawater in duplicate baffled recirculation tanks (BRT)
402 and allowing the oil and seawater to mix for ~24 h (55). Mesocosm tanks were then filled
403 by withdrawing WAF from the bottom of the recirculation tanks in order to avoid including
404 any non-accommodated oil floating on the surface of the BRTs. Because the concentration
405 of oil in the CEWAF treatment was so high, we included the DCEWAF treatment in order to
406 observe the effects of a chemically dispersed oil, but at a concentration more commonly
407 encountered at sea after an oil spill (56). Each mesocosm tank contained 90L of seawater
408 supplemented at the start of the experiment with nutrients (N, P, Si) prepared using the
409 Guillard and Ryther recipe for f/20 media (57) . This was done to ensure microbial
410 communities would not be nutrient limited during the experiment. Full-spectrum

411 fluorescent lamps (UV-Vis 375-750nm; Sylvania GRO-LUX; Wilmington, MA, USA) provided
412 a 12h light/12h dark cycle (50-80 μmol photons m^{-2} s^{-1}) and the room was kept at ~21°C.
413 Each mesocosm experiment was run until the remaining oil concentration within
414 the CEWAF treatment (highest oil concentration) reached ~20% of the initial oil
415 concentration (58, 59). This was 72h and 96h for the Coastal and Offshore experiments,
416 respectively. For each experiment, starting at time zero and every 12h thereafter, ~1L of
417 water was collected from each mesocosm in a clean, opaque Nalgene bottle through a
418 PTFE-lined spigot mounted on the side of each tank (10cm above bottom). For cell count
419 samples, 10mL of this water was fixed with formalin (final concentration 2%) and stored at
420 4°C. For DNA samples, the collected water was prefiltered through a 10μm filter to exclude
421 zooplankton and large eukaryotic cells followed by filtering 200mL onto a 47mm, 0.22μm
422 Supor PES membrane (Pall; Port Washington, NY, USA). For RNA samples, up to 800mL (or
423 until clogged) of the remaining 10μm-prefiltered water was filtered onto 47mm, 0.22μm
424 Supor PES membranes. After collection, all filters were placed in cryotubes and stored at -
425 80°C. RNA filters were immersed in 1mL of TE buffer (10mM Tris, 1mM EDTA, pH 7.5)
426 before freezing.

427 **Analysis of hydrocarbon chemistry**

428 Samples (1-3.5 L) were collected every 24 hours in amber bottles with Teflon lined
429 screw caps from each of the triplicate treatment tanks and immediately amended with
430 ~20mL of dichloromethane (DCM). Prior to extraction, PAH surrogates (d8-naphthalene,
431 d10-acenaphthene, d10-phenanthrene, d12-chrysene, and d12-perylene) and aliphatic
432 surrogate standards (deuterated nC12, nC20, nC24, and nC30) were added (60). The DCM
433 mixture was reduced, exchanged into hexane, and then transferred to silica gel/alumina

434 columns for purification (59). Hydrocarbons were eluted with 200 ml of a 1:1
435 pentane/DCM solution, evaporated, and exchanged with hexane (61, 62). Aliphatic
436 hydrocarbons were then analyzed on an Agilent 7890 gas chromatograph with a flame
437 ionization detector (GC/FID) according to Wade et al. (61) with updates in Morales-
438 McDevitt et al. (60). PAHs were analyzed on a Hewlett-Packard 6890 gas chromatograph
439 coupled with a Hewlett-Packard 5973 mass selective detector. A laboratory reference
440 sample was analyzed with each batch of samples to confirm GC/MS/SIM system
441 performance and calibration (61, 62). Alkylated PAH were quantitated based response of
442 the parent PAH compound (60).

443 **16S rRNA Gene Amplicon Sequencing**

444 The V4 hyper-variable region of the 16S rRNA gene was amplified from each sample
445 following the protocol previously described in Doyle et al. (34). Briefly, filters were sliced
446 into small pieces using a sterile scalpel and subsequently extracted using FastDNA Spin kits
447 (MP Biomedical; Santa Ana, CA, USA). Five sample-free filters were processed as protocol
448 blanks. Universal (Bacteria and Archaea) V4 primers 515F and 806R primers were used for
449 amplification (63) . Sequencing was performed on the Illumina MiSeq platform (500 cycle,
450 V2 chemistry) at the Georgia Genomics Facility (Athens, GA, USA). Raw read curation and
451 processing into amplicon sequence variants (ASVs) was performed by following the
452 standard pipeline of the DADA2 package (64) in R (see Supplementary Methods; Figure
453 S9). All ASV tables were subsampled without replacement to an even depth (Table S3)
454 before downstream ecological analyses were performed with a combination of mothur
455 v1.42.1, phyloseq v1.28, and/or vegan v.2.5-6 (65–67).

456 **Redundancy Analysis**

457 Redundancy analyses (RDA) were performed to investigate the relationship
458 between microbial community compositions, hours of incubation, and initial oil
459 concentrations and to identify ASVs associated with the presence of oil. For these analyses,
460 ASVs without an average relative abundance ≥0.2% in at least one sample were excluded.
461 ASV counts were normalized using a Hellinger transformation to transform the abundance
462 data into a Euclidean space (68). The significance of each RDA model was assessed using a
463 permutational ANOVA test (69) and the variance explained by each variable (i.e. hours and
464 initial oil concentration) was estimated by variance partitioning with partial RDAs (70).
465 ASVs associated with the presence of oil were identified as those whose RDA-weighted
466 average loading scores were positively correlated with the presence of oil and were greater
467 than the equilibrium contribution of the RDA model (the proportion of variance which
468 would be explained by a random canonical axis).

469 **RNA Extraction and Metatranscriptome Sequencing**

470 For each mesocosm experiment, three time points, corresponding to the start,
471 middle, and end of the experiment, were selected for metatranscriptomic sequencing (0h,
472 36h, and 72h for the Coastal experiment, and 0h, 48h, and 96h for the Offshore
473 experiment). To ensure an adequate quantity of RNA was recovered for sequencing, the
474 triplicate samples for each treatment were combined into a single extraction. A customized
475 phenol:chloroform RNA extraction was used to isolate RNA; details are given in
476 Supplementary Methods. Genomic DNA was eliminated from RNA samples with TURBO
477 DNA-free kits (Ambion; Waltham, MA, USA) followed by purification with MEGAclear
478 Transcription Clean-up kits (Ambion). The resulting purified total RNA extracts were
479 processed with MICROBExpress kits (Ambion) to reduce the amount of 16S and 23S rRNA

480 transcripts within the samples and then sent to the University of Delaware DNA
481 Sequencing & Genotyping Center (Newark, DE, USA) for Illumina HiSeq 2500 sequencing
482 (paired-end 150bp reads).

483 **Metatranscriptome analysis**

484 De novo transcriptome assembly was performed with the curated paired reads (see
485 Supplementary Methods for details) using Trinity v2.5.1 (71) with default parameters,
486 producing 648 351 contigs ranging between 201 and 54 422 bp in length. Contig
487 abundances within each sample were then quantified by mapping reads to the
488 metatranscriptome assembly with kallisto v0.44.0 (72). Read counts were normalized for
489 contig length into TPM (transcripts per million transcripts) values as previously described
490 (73), and scaled for cross-sample comparison using the trimmed mean of M-values (TMM)
491 method described by Robinson and Oshlack (74). Open reading frames were identified and
492 translated into amino acid sequences using Prodigal v2.6.3 in anonymous mode (75).
493 Functional annotations were performed using a GHOSTX v1.3.7 search against the Kyoto
494 Encyclopedia of Genes and Genomes (KEGG) database using the single-directional best hit
495 assignment method targeted to prokaryotes. A custom R script was then used to select all
496 transcripts whose functional annotation belonged to a KEGG pathway involved in the
497 degradation of saturated hydrocarbons (alkanes and cycloalkanes), PAHs, or their
498 metabolic intermediates to central metabolism (glycolysis, TCA cycle) substrates (Table
499 S7). We also searched for genes involved in the initial oxidation of alkanes using a BLASTP
500 (single best hit $\leq 1E^{-20}$, alignment length ≥ 100, bit score ≥ 50) search of a custom database
501 (Table S8) of soluble cytochrome P450 alkane hydroxylases of the CYP153 family (45).
502 These proteins would have been missed from the above KEGG-based analysis as there are

503 currently no KEGG orthologs specific to this family of enzymes (76). Identified
504 hydrocarbon degradation gene transcripts were taxonomically classified using KAIJU v1.6.3
505 in greedy mode (5 substitutions allowed) with the NCBI non-redundant database
506 (+eukaryotes) as a reference (77). Transcripts with identically scored matches to different
507 taxa were classified to the least common ancestor in the phylogenetic tree. Following the
508 method described in Jenior et al. (78), an outlier analysis was performed to estimate the
509 number of highly expressed transcripts within each sample.

510 ACKNOWLEDGMENTS

511 Data is publicly available through the Gulf of Mexico Research Initiative Information
512 and Data Cooperative (GRIIDC) at http://data.gulfresearchinitative.org DOIs:
513 10.7266/N77D2SPZ (Coastal 16S rRNA libraries), 10.7266/N7C53JDP (Offshore 16S rRNA
514 libraries), 10.7266/9EDJRA3Q (metatranscriptome sequences), 10.7266/N74X568X
515 (Coastal alkane and PAH measurements), and 10.7266/N78P5XZD (Offshore alkane and
516 PAH measurements).

517 FUNDING INFORMATION

518 This research was made possible by a grant from The Gulf of Mexico Research
519 Initiative to support consortium research entitled ADDOMEx (Aggregation and Degradation
520 of Dispersants and Oil by Microbial Exopolymers) and the ADDOMEx-2 Consortia.

521 REFERENCES

522 1. Tissot BP, Welte DH. 1984. Petroleum formation and occurrence, 2nd ed. Springer: Berlin,
523 Heidelberg, Germany.

524 2. Head IM, Jones DM, Röling WFM. 2006. Marine microorganisms make a meal of oil. Nature
525 Reviews Microbiology 4:173–182.

526 3. Lessard RR, DeMarco G. 2000. The Significance of Oil Spill Dispersants. Spill Science &
527 Technology Bulletin 6:59–68.

528 4. Brakstad OG, Ribicic D, Winkler A, Netzer R. 2018. Biodegradation of dispersed oil in seawater
529 is not inhibited by a commercial oil spill dispersant. Marine Pollution Bulletin 129:555–561.

530 5. Hamdan L, Fulmer P. 2011. Effects of COREXIT® EC9500A on bacteria from a beach oiled by
531 the Deepwater Horizon spill. Aquatic Microbial Ecology 63:101–109.

532 6. Kleindienst S, Seidel M, Ziervogel K, Grim S, Loftis K, Harrison S, Malkin SY, Perkins MJ, Field J,
533 Sogin ML, Dittmar T, Passow U, Medeiros PM, Joye SB. 2015. Chemical dispersants can
534 suppress the activity of natural oil-degrading microorganisms. Proceedings of the National
535 Academy of Sciences 112:14900–14905.

536 7. Techtmann SM, Zhuang M, Campo P, Holder E, Elk M, Hazen TC, Conmy R, Domingo JWS. 2017.
537 Corexit 9500 Enhances Oil Biodegradation and Changes Active Bacterial Community Structure
538 of Oil-Enriched Microcosms. Appl Environ Microbiol 83:e03462-16.

539 8. Tremblay J, Yergeau E, Fortin N, Cobanli S, Elias M, King TL, Lee K, Greer CW. 2017. Chemical
540 dispersants enhance the activity of oil-and gas condensate-degrading marine bacteria. The
541 ISME Journal.

542 9. Atlas RM, Hazen TC. 2011. Oil Biodegradation and Bioremediation: A Tale of the Two Worst
543 Spills in U.S. History. Environmental Science & Technology 45:6709–6715.

544 10. Kujawinski EB, Kido Soule MC, Valentine DL, Boysen AK, Longnecker K, Redmond MC. 2011.
545 Fate of Dispersants Associated with the Deepwater Horizon Oil Spill. Environ Sci Technol
546 45:1298–1306.

547 11. Dubinsky EA, Conrad ME, Chakraborty R, Bill M, Borglin SE, Hollibaugh JT, Mason OU, M.
548 Piceno Y, Reid FC, Stringfellow WT, Tom LM, Hazen TC, Andersen GL. 2013. Succession of
549 Hydrocarbon-Degrading Bacteria in the Aftermath of the *Deepwater Horizon* Oil Spill in the
550 Gulf of Mexico. Environmental Science & Technology 47:10860–10867.

551 12. Gutierrez T, Singleton DR, Berry D, Yang T, Aitken MD, Teske A. 2013. Hydrocarbon-degrading
552 bacteria enriched by the Deepwater Horizon oil spill identified by cultivation and DNA-SIP.
553 The ISME journal 7:2091.

554 13. Hazen TC, Dubinsky EA, DeSantis TZ, Andersen GL, Piceno YM, Singh N, Jansson JK, Probst A,
555 Borglin SE, Fortney JL, Stringfellow WT, Bill M, Conrad ME, Tom LM, Chavarria KL, Alusi TR,
556 Lamendella R, Joyner DC, Spier C, Baelum J, Auer M, Zemla ML, Chakraborty R, Sonnenthal EL,
557 D'haeseleer P, Holman H-YN, Osman S, Lu Z, Nostrand JDV, Deng Y, Zhou J, Mason OU. 2010.
558 Deep-Sea Oil Plume Enriches Indigenous Oil-Degrading Bacteria. Science 330:204–208.

559 14. Mason OU, Hazen TC, Borglin S, Chain PS, Dubinsky EA, Fortney JL, Han J, Holman H-YN,
560 Hultman J, Lamendella R, others. 2012. Metagenome, metatranscriptome and single-cell
561 sequencing reveal microbial response to Deepwater Horizon oil spill. The ISME journal
562 6:1715–1727.

563 15. Rivers AR, Sharma S, Tringe SG, Martin J, Joye SB, Moran MA. 2013. Transcriptional response
564 of bathypelagic marine bacterioplankton to the Deepwater Horizon oil spill. The ISME journal
565 7:2315–2329.

566 16. Engel AS, Gupta AA. 2014. Regime Shift in Sandy Beach Microbial Communities following
567 Deepwater Horizon Oil Spill Remediation Efforts. PLoS ONE 9:e102934.

568 17. Kostka JE, Prakash O, Overholt WA, Green SJ, Freyer G, Canion A, Delgardio J, Norton N, Hazen
569 TC, Huettel M. 2011. Hydrocarbon-Degrading Bacteria and the Bacterial Community Response
570 in Gulf of Mexico Beach Sands Impacted by the Deepwater Horizon Oil Spill. Applied and
571 Environmental Microbiology 77:7962–7974.

572 18. Lamendella R, Strutt S, Borglin SE, Chakraborty R, Tas N, Mason OU, Hultman J, Prestat E,
573 Hazen TC, Jansson J. 2014. Assessment of the Deepwater Horizon oil spill impact on Gulf coast
574 microbial communities. Front Microbiol 5.

575 19. Rodriguez-r LM, Overholt WA, Hagan C, Huettel M, Kostka JE, Konstantinidis KT. 2015.
576 Microbial community successional patterns in beach sands impacted by the Deepwater
577 Horizon oil spill. The ISME journal.

578 20. Beazley MJ, Martinez RJ, Rajan S, Powell J, Piceno YM, Tom LM, Andersen GL, Hazen TC, Van
579 Nostrand JD, Zhou J, Mortazavi B, Sobecky PA. 2012. Microbial Community Analysis of a
580 Coastal Salt Marsh Affected by the Deepwater Horizon Oil Spill. PLoS ONE 7:e41305.

581 21. Mahmoudi N, Porter TM, Zimmerman AR, Fulthorpe RR, Kasozi GN, Silliman BR, Slater GF.
582 2013. Rapid Degradation of Deepwater Horizon Spilled Oil by Indigenous Microbial
583 Communities in Louisiana Saltmarsh Sediments. Environ Sci Technol 47:13303–13312.

584 22. King GM, Kostka JE, Hazen TC, Sobecky PA. 2015. Microbial Responses to the *Deepwater*
585 *Horizon* Oil Spill: From Coastal Wetlands to the Deep Sea. Annual Review of Marine Science
586 7:377–401.

587 23. Fortunato CS, Crump BC. 2011. Bacterioplankton Community Variation Across River to Ocean
588 Environmental Gradients. Microb Ecol 62:374–382.

589 24. D'Ambrosio L, Ziervogel K, MacGregor B, Teske A, Arnosti C. 2014. Composition and enzymatic
590 function of particle-associated and free-living bacteria: a coastal/offshore comparison. The
591 ISME Journal 8:2167–2179.

592 25. Watson SW, Novitsky TJ, Quinby HL, Valois FW. 1977. Determination of bacterial number and
593 biomass in the marine environment. Applied and Environmental Microbiology 33:940–946.

594 26. Bianchi A, Giuliano L. 1996. Enumeration of viable bacteria in the marine pelagic environment.
595 Applied and environmental microbiology 62:174–177.

596 27. Gutierrez T, Green DH, Nichols PD, Whitman WB, Semple KT, Aitken MD. 2013.
597 Polycyclovorans algicola gen. nov., sp. nov., an Aromatic-Hydrocarbon-Degrading Marine
598 Bacterium Found Associated with Laboratory Cultures of Marine Phytoplankton. Applied and
599 Environmental Microbiology 79:205–214.

600 28. Van Beilen JB, Li Z, Duetz WA, Smits THM, Witholt B. 2003. Diversity of Alkane Hydroxylase
601 Systems in the Environment. Oil & Gas Science and Technology 58:427–440.

602 29. Johnsen AR, Wick LY, Harms H. 2005. Principles of microbial PAH-degradation in soil.
603 Environmental Pollution 133:71–84.

604 30. Seo J-S, Keum Y-S, Li QX. 2009. Bacterial Degradation of Aromatic Compounds. Int J Environ
605 Res Public Health 6:278–309.

606 31. Dyksterhouse SE, Gray JP, Herwig RP, Lara JC, Staley JT. 1995. Cycloclasticus pugetii gen. nov.,
607 sp. nov., an aromatic hydrocarbon-degrading bacterium from marine sediments. International
608 Journal of Systematic and Evolutionary Microbiology 45:116–123.

609 32. Yakimov MM, Timmis KN, Golyshin PN. 2007. Obligate oil-degrading marine bacteria. Current
610 Opinion in Biotechnology 18:257–266.

611 33. Orcutt BN, Joye SB, Kleindienst S, Knittel K, Ramette A, Reitz A, Samarkin V, Treude T, Boetius
612 A. 2010. Impact of natural oil and higher hydrocarbons on microbial diversity, distribution,
613 and activity in Gulf of Mexico cold-seep sediments. Deep Sea Research Part II: Topical Studies
614 in Oceanography 57:2008–2021.

615 34. Doyle SM, Whitaker EA, De Pascuale V, Wade TL, Knap AH, Santschi PH, Quigg A, Sylvan JB.
616 2018. Rapid Formation of Microbe-Oil Aggregates and Changes in Community Composition in
617 Coastal Surface Water Following Exposure to Oil and the Dispersant Corexit. Front Microbiol
618 9.

619 35. Redmond MC, Valentine DL. 2012. Natural gas and temperature structured a microbial
620 community response to the Deepwater Horizon oil spill. Proceedings of the National Academy
621 of Sciences 109:20292–20297.

622 36. Wang W, Zhong R, Shan D, Shao Z. 2014. Indigenous oil-degrading bacteria in crude oil-
623 contaminated seawater of the Yellow sea, China. Applied Microbiology and Biotechnology
624 98:7253–7269.

625 37. Jin HM, Kim JM, Lee HJ, Madsen EL, Jeon CO. 2012. Alteromonas As a Key Agent of Polycyclic
626 Aromatic Hydrocarbon Biodegradation in Crude Oil-Contaminated Coastal Sediment. Environ
627 Sci Technol 46:7731–7740.

628 38. McGenity TJ, Folwell BD, McKew BA, Sanni GO. 2012. Marine crude-oil biodegradation: a
629 central role for interspecies interactions. Aquatic Biosystems 8:10.

630 39. Iwaki H, Yamamoto T, Hasegawa Y. 2018. Isolation of marine xylene-utilizing bacteria and
631 characterization of Halioxenophilus aromaticivorans gen. nov., sp. nov. and its xylene
632 degradation gene cluster. FEMS Microbiol Lett 365.

633 40. Rojo F. 2009. Degradation of alkanes by bacteria. Environmental Microbiology 11:2477–2490.

634 41. Das N, Chandran P. 2011. Microbial Degradation of Petroleum Hydrocarbon Contaminants: An
635 Overview. Biotechnology Research International 2011:1–13.

636 42. Sugiura K, Ishihara M, Shimauchi T, Harayama S. 1997. Physicochemical Properties and
637 Biodegradability of Crude Oil. Environ Sci Technol 31:45–51.

638 43. Wang Z, Fingas M, Blenkinsopp S, Sergy G, Landriault M, Sigouin L, Foght J, Semple K, Westlake
639 DWS. 1998. Comparison of oil composition changes due to biodegradation and physical
640 weathering in different oils. Journal of Chromatography A 809:89–107.

641 44. Jonker MTO, Brils JM, Sinke AJC, Murk AJ, Koelmans AA. 2006. Weathering and toxicity of
642 marine sediments contaminated with oils and polycyclic aromatic hydrocarbons.
643 Environmental Toxicology and Chemistry 25:1345–1353.

644 45. Nie Y, Chi C-Q, Fang H, Liang J-L, Lu S-L, Lai G-L, Tang Y-Q, Wu X-L. 2014. Diverse alkane
645 hydroxylase genes in microorganisms and environments. Scientific Reports 4:4968.

646 46. Yakimov MM. 2004. Thalassolituus oleivorans gen. nov., sp. nov., a novel marine bacterium
647 that obligately utilizes hydrocarbons. INTERNATIONAL JOURNAL OF SYSTEMATIC AND
648 EVOLUTIONARY MICROBIOLOGY 54:141–148.

649 47. Teramoto M, Ohuchi M, Hatmanti A, Darmayati Y, Widyastuti Y, Harayama S, Fukunaga Y.
650 2011. Oleibacter marinus gen. nov., sp. nov., a bacterium that degrades petroleum aliphatic
651 hydrocarbons in a tropical marine environment. International Journal of Systematic and
652 Evolutionary Microbiology 61:375–380.

653 48. White HK, Marx CT, Valentine DL, Sharpless CM, Aeppli C, Gosselin K, Kivenson V, Liu RM,
654 Nelson RK, Sylva SP, Reddy CM. 2019. Examining inputs of biogenic and oil-derived
655 hydrocarbons in surface waters following the Deepwater Horizon oil spill. ACS Earth Space
656 Chem acsearthspacechem.9b00090.

657 49. Lea-Smith DJ, Biller SJ, Davey MP, Cotton CAR, Sepulveda BMP, Turchyn AV, Scanlan DJ, Smith
658 AG, Chisholm SW, Howe CJ. 2015. Contribution of cyanobacterial alkane production to the
659 ocean hydrocarbon cycle. PNAS 112:13591–13596.

660 50. Valentine DL, Reddy CM. 2015. Latent hydrocarbons from cyanobacteria. PNAS 112:13434–
661 13435.

662 51. Li N, Chang W, Warui DM, Booker SJ, Krebs C, Bollinger JM. 2012. Evidence for Only
663 Oxygenative Cleavage of Aldehydes to Alk(a/e)nes and Formate by Cyanobacterial Aldehyde
664 Decarbonylases. Biochemistry 51:7908–7916.

665 52. Jiménez-Díaz L, Caballero A, Pérez-Hernández N, Segura A. 2017. Microbial alkane production
666 for jet fuel industry: motivation, state of the art and perspectives. Microbial Biotechnology
667 10:103–124.

668 53. Singh AK, Sherry A, Gray ND, Jones DM, Bowler BFJ, Head IM. 2014. Kinetic parameters for
669 nutrient enhanced crude oil biodegradation in intertidal marine sediments. Front Microbiol 5.

670 54. Teira E, Lekunberri I, Gasol JM, Nieto-Cid M, Álvarez-Salgado XA, Figueiras FG. 2007. Dynamics
671 of the hydrocarbon-degrading Cycloclasticus bacteria during mesocosm-simulated oil spills.
672 Environmental Microbiology 9:2551–2562.

673 55. Knap AH, Sleeter TD, Dodge RE, Wyers SC, Frith HR, Smith SR. 1983. The effects of oil spills
674 and dispersant use on corals: a review and multidisciplinary experimental approach. Oil and
675 Petrochemical Pollution 1:157–169.

676 56. Lee K, Nedwed T, Prince RC, Palandro D. 2013. Lab tests on the biodegradation of chemically
677 dispersed oil should consider the rapid dilution that occurs at sea. Marine Pollution Bulletin
678 73:314–318.

679 57. Guillard RRL, Ryther JH. 1962. STUDIES OF MARINE PLANKTONIC DIATOMS: I. CYCLOTELLA
680 NANA HUSTEDT, AND DETONULA CONFERVACEA (CLEVE) GRAN. Canadian Journal of
681 Microbiology 8:229–239.

682 58. Kamalanathan M, Xu C, Schwehr K, Bretherton L, Beaver M, Doyle SM, Genzer J, Hillhouse J,
683 Sylvan JB, Santschi P, Quigg A. 2018. Extracellular Enzyme Activity Profile in a Chemically
684 Enhanced Water Accommodated Fraction of Surrogate Oil: Toward Understanding Microbial
685 Activities After the Deepwater Horizon Oil Spill. Front Microbiol 9.

686 59. Xu C, Lin P, Zhang S, Sun L, Xing W, Schwehr KA, Chin W-C, Wade TL, Knap AH, Hatcher PG,
687 Yard A, Jiang C, Quigg A, Santschi PH. 2019. The interplay of extracellular polymeric
688 substances and oil/Corexit to affect the petroleum incorporation into sinking marine oil snow
689 in four mesocosms. Science of The Total Environment 693:133626.

690 60. Morales-McDevitt M, Shi D, Knap AH, Quigg A, Sweet ST, Sericano JL, Wade TL. in review. Fate
691 and transport of petroleum hydrocarbons in controlled mesocosm studies. PLOS ONE.

692 61. Wade TL, Sweet ST, Sericano JL, Guinasso NL, Diercks A-R, Highsmith RC, Asper VL, Joung D,
693 Shiller AM, Lohrenz SE, Joye SB. 2011. Analyses of Water Samples From the Deepwater
694 Horizon Oil Spill: Documentation of the Subsurface Plume, p. 77–82. *In* Liu, Y, MacFadyen, A, Ji,
695 Z-G, Weisberg, RH (eds.), Geophysical Monograph Series. American Geophysical Union,
696 Washington, D. C.

697 62. Wade TL, Sericano JL, Sweet ST, Knap AH, Guinasso NL. 2016. Spatial and temporal
698 distribution of water column total polycyclic aromatic hydrocarbons (PAH) and total
699 petroleum hydrocarbons (TPH) from the Deepwater Horizon (Macondo) incident. Marine
700 Pollution Bulletin 103:286–293.

701 63. Walters W, Hyde ER, Berg-Lyons D, Ackermann G, Humphrey G, Parada A, Gilbert JA, Jansson
702 JK, Caporaso JG, Fuhrman JA, others. 2016. Improved bacterial 16S rRNA gene (V4 and V4-5)
703 and fungal internal transcribed spacer marker gene primers for microbial community surveys.
704 mSystems 1:e00009–15.

705 64. Callahan BJ, McMurdie PJ, Rosen MJ, Han AW, Johnson AJA, Holmes SP. 2016. DADA2: High-
706 resolution sample inference from Illumina amplicon data. Nature Methods 13:581–583.

707 65. McMurdie PJ, Holmes S. 2013. phyloseq: An R Package for Reproducible Interactive Analysis
708 and Graphics of Microbiome Census Data. PLOS ONE 8:e61217.

709 66. Oksanen J, Blanchet FG, Friendly M, Kindt R, Legendre P, McGlinn D, Minchin PR, O'Hara RB,
710 Simpson GL, Solymos P, Stevens MHH, Szoecs E, Wagner H. 2018. vegan: Community Ecology
711 Package.

712 67. Schloss PD, Westcott SL, Ryabin T, Hall JR, Hartmann M, Hollister EB, Lesniewski RA, Oakley
713 BB, Parks DH, Robinson CJ, Sahl JW, Stres B, Thallinger GG, Horn DJV, Weber CF. 2009.

714 Introducing mothur: Open-Source, Platform-Independent, Community-Supported Software for
715 Describing and Comparing Microbial Communities. Appl Environ Microbiol 75:7537–7541.

716 68. Legendre P, Gallagher ED. 2001. Ecologically meaningful transformations for ordination of
717 species data. Oecologia 129:271–280.

718 69. Legendre P, Oksanen J, Braak CJF ter. 2011. Testing the significance of canonical axes in
719 redundancy analysis. Methods in Ecology and Evolution 2:269–277.

720 70. Legendre P, Borcard D, Roberts DW. 2012. Variation partitioning involving orthogonal spatial
721 eigenfunction submodels. Ecology 93:1234–1240.

722 71. Grabherr MG, Haas BJ, Yassour M, Levin JZ, Thompson DA, Amit I, Adiconis X, Fan L,
723 Raychowdhury R, Zeng Q, Chen Z, Mauceli E, Hacohen N, Gnirke A, Rhind N, Palma F di, Birren
724 BW, Nusbaum C, Lindblad-Toh K, Friedman N, Regev A. 2011. Full-length transcriptome
725 assembly from RNA-Seq data without a reference genome. Nature Biotechnology 29:644–652.

726 72. Bray NL, Pimentel H, Melsted P, Pachter L. 2016. Near-optimal probabilistic RNA-seq
727 quantification. Nature Biotechnology 34:525–527.

728 73. Wagner GP, Kin K, Lynch VJ. 2012. Measurement of mRNA abundance using RNA-seq data:
729 RPKM measure is inconsistent among samples. Theory Biosci 131:281–285.

730 74. Robinson MD, Oshlack A. 2010. A scaling normalization method for differential expression
731 analysis of RNA-seq data. Genome Biology 11:R25.

732 75. Hyatt D, Chen G-L, LoCascio PF, Land ML, Larimer FW, Hauser LJ. 2010. Prodigal: prokaryotic
733 gene recognition and translation initiation site identification. BMC Bioinformatics 11:119.

734 76. Tremblay J, Greer C. 2019. Metagenomic Data Mining in Oil Spill Studies, p. 211–223. *In*
735 Comprehensive Biotechnology 3rd Edition. Pergamon.

736 77. Menzel P, Ng KL, Krogh A. 2016. Fast and sensitive taxonomic classification for metagenomics
737 with Kaiju. Nature Communications 7:11257.

738 78. Jenior ML, Leslie JL, Young VB, Schloss PD. 2018. *Clostridium difficile* Alters the Structure and
739 Metabolism of Distinct Cecal Microbiomes during Initial Infection To Promote Sustained
740 Colonization. mSphere 3:e00261-18, /msphere/3/3/mSphere261-18.atom.

741
742
743
744
745
746
747
748
749
750
751
752
753
754
755
756
757
758
759
760
761
762

763 **FIGURE LEGENDS**

764 **Figure 1.** Measured concentrations (μg/L) of total alkanes and total PAHs over time in both
765 mesocosm experiments. Error bars denote standard deviation.

766

767 **Figure 2.** Relative abundances of abundant microbial lineages observed in each
768 experiment. Each bar is the average of triplicate treatments. Community composition in the
769 original seawater samples collected for each experiment are shown under category "SW".
770 The plot was built to display the highest resolution classification for the most abundant
771 taxa. The plot was constructed as follows: First, ASVs were clustered at the genus level and
772 any genera having a relative abundance ≥15% in at least one of the samples were plotted.
773 This procedure was subsequently repeated with the remaining unplotted ASVs at the
774 taxonomic levels of family, order, class and phylum. Any remaining rare ASVs left after this
775 procedure were not plotted.

776

777 **Figure 3.** Heatmap displaying the relative abundances of the 30 ASVs identified as being
778 oil-enriched using the RDA models. ASVs identified in both experiments are highlighted
779 with a gray bar. Colored stars on the left side indicate the treatment(s) in which an ASV's
780 relative abundance over time was significantly enriched versus the Control. ASV read
781 counts were transformed with a Hellinger transformation in order to facilitate a clearer
782 visual comparison between abundant and sparse taxa.

783

784

785 **Figure 4.** Coastal and offshore microbial communities exhibited differential expression of
786 alkane and PAH catabolic pathways after exposure to oil. Taxonomic affiliations and
787 abundances of hydrocarbon degradation gene transcripts are shown within four metabolic
788 categories. Y-axes are individually scaled for each category (row). Transcripts belonging to
789 minor taxa (<2% total abundance) were removed for clarity.
790
791 **Figure 5.** Summary overview of the taxonomic distribution and summed abundances,
792 between all four treatments, of expressed hydrocarbon degradation genes involved in the
793 transformation of n-alkanes (orange arrows) and PAHs (green arrows) to central
794 metabolism intermediates.
795
796 **Figure 6.** Alpha diversity of hydrocarbon degradation gene transcripts within the four
797 metabolic categories. Transcripts within each category were taxonomically classified using
798 KAIJU (minimum score 65) and then clustered by genus before calculating Inverse-Simpson
799 indices.
800

801 ## LEGENDS FOR SUPPLEMENTAL MATERIAL

802 **Figure S1.** Map showing the locations where seawater for the Coastal and Offshore
803 experiments were collected.
804
805 **Figure S2.** Observed cell abundances with each treatment of the Coastal and Offshore
806 experiments. Error bars denote standard deviations.
807

808 **Figure S3.** (A, E) NMDS ordination of Bray-Curtis dissimilarities in the Offshore and Coastal
809 experiments indicated microbial community structure was driven by the level of oil
810 exposure (treatment). Numbered labels indicate hours of incubation. (B-D and F-H) RDA
811 score triplots for the three oil-amended treatments within the Offshore and Coastal
812 experiments, respectively. Each treatment was modeled against the Control. Colored circles
813 represent samples. Plus (+) signs represent ASVs. Purple rings represent the equilibrium
814 contribution of the overall model. Arrows represent the vectors of the two explanatory
815 variables used in the model: (1) the presence of oil, and (2) hours of incubation. Right-
816 angled scalar projections of an ASV point onto the oil vector approximates that ASV's
817 association with the presence of oil. Bolded, red ASVs were designated as oil-associated for
818 this study.
819
820 **Figure S4.** Relative abundances of abundant microbial lineages observed in each
821 experiment based on the metatranscriptomes. The plot was built to display the highest
822 resolution classification for the most abundant taxa. The plot was constructed as follows:
823 First, transcripts were clustered at the genus level and any genera having a relative
824 abundance ≥20% in at least one of the samples were plotted. This procedure was
825 subsequently repeated with the remaining unplotted transcripts at the taxonomic levels of
826 family, order, class and phylum. Any remaining rare transcripts left after this procedure
827 were not plotted.
828
829 **Figure S5.** Observed variation in the relative abundance of the 10 most abundant orders in
830 the 16S rRNA amplicon dataset. Cross-lines indicated the median observed relative

831 abundance. Larger boxes indicate increased variability over time with that respective
832 treatment.
833
834 **Figure S6.** Outlier analysis of hydrocarbon degradation gene expression within the Coastal
835 WAF, DCEWAF, and CEWAF treatments versus the Control treatments. Each point
836 represents a unique open reading frame identified in the respective metatranscriptomes.
837 Outliers were defined using a squared residual cutoff value of 2 versus the x = y dotted-line.
838 Points are colored by taxonomic assignment (genus) of each transcript. Gray points denote
839 those genes whose abundance were comparable between the respective oil-amended
840 treatment and the Control. Outliers above the shaded-gray ribbon were considered highly
841 expressed. Outlier analysis was performed using a modification of the custom R-scripts
842 described in Jenior et al. (2018).
843
844 **Figure S7.** Outlier analysis of hydrocarbon degradation gene expression within the
845 Offshore WAF, DCEWAF, and CEWAF treatments versus the Control treatments. Each point
846 represents a unique open reading frame identified in the respective metatranscriptomes.
847 Outliers were defined using a squared residual cutoff value of 2 versus the x = y dotted-line.
848 Points are colored by taxonomic assignment (genus) of each transcript. Gray points denote
849 those genes whose abundance were comparable between the respective oil-amended
850 treatment and the Control. Outliers above the shaded-gray ribbon were considered highly
851 expressed. Outlier analysis was performed using a modification of the custom R-scripts
852 described in Jenior et al. (2018).
853

854 **Figure S8.** Hydrocarbon degradation genes were identified by comparing their abundance
855 in each oil-amended treatment with that observed in the respective Control. Although the
856 number of upregulated genes differed between treatments (see Figure S6 and S6), the
857 amount those genes were upregulated did not differ between treatment.
858
859 **Figure S9.** Rarefaction curves for all 16S ASV libraries reached saturation.
860
861 **Table S1.** Seawater samples collected for mesocosm experiments.
862
863 **Table S2.** Measured concentrations (μg/L) of total alkanes and total PAHs over time in
864 both mesocosm experiments. Half-lifes (t0.5) were calculated over 72 hours. %RSD
865 denotes the relative standard deviation. n.d. indicates half-life not determined.
866
867 **Table S3.** Alpha Diversity Summary of 16S rRNA amplicon libraries. (* denotes values
868 calculated after normalizing read-depth by subsampling each library to 7754 reads; 1000
869 iterations)
870
871 **Table S4.** Number of sequence reads that made it through each step of the DADA2 pipeline.
872
873 **Table S5.** Read count within each sample, taxonomy, and sequence of each ASV.
874
875 **Table S6.** Metatranscriptome reads identifed as rRNA using SortMeRNA
876

877 **Table S7.** All transcripts whose KEGG annotation, generated using GHOSTX, matched one

878 of the following were identified as hydrocarbon degradation gene transcripts

879

880 **Table S8.** List of proteins in our CYP153 database. We used this database along with

881 BLASTP to identify transcripts for P450 alkane hydroxylases of the CYP153 family.

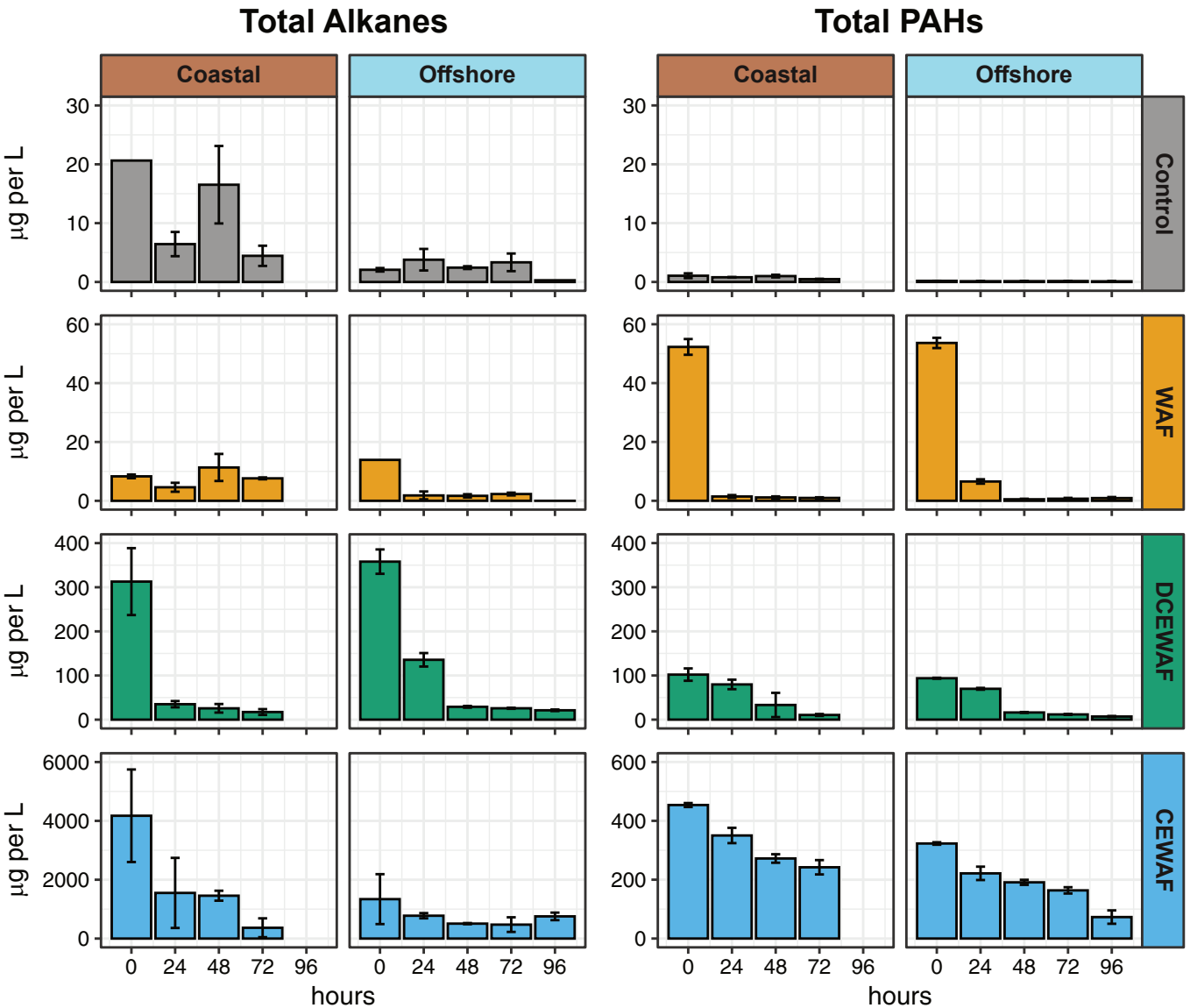
Total Alkanes
Total PAHs
Coastal
Offshore
Coastal
Offshore
Control
WAF
DCEWAF
CEWAF
µg per L
hours
hours
0
24
48
72
96

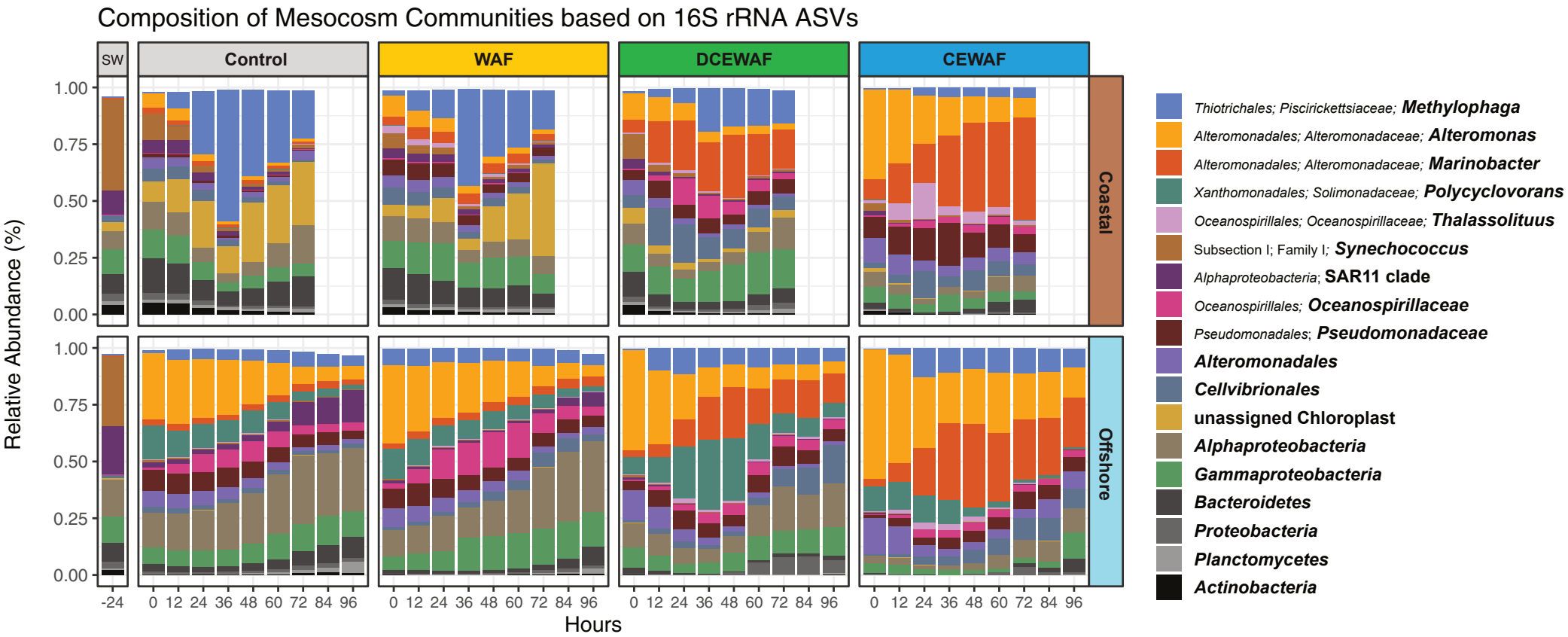
Composition of Mesocosm Communities based on 16S rRNA ASVs
SW
Control
WAF
DCEWAF
CEWAF
Coastal
Offshore
Relative Abundance (%)
1.00
0.75
0.50
0.25
0.00
-24
0 12 24 36 48 60 72 84 96
Hours
Thiotrichales; Piscirickettsiaceae; Methylophaga
Alteromonadales; Alteromonadaceae; Alteromonas
Alteromonadales; Alteromonadaceae; Marinobacter
Xanthomonadales; Solimonadaceae; Polycyclovorans
Oceanospirillales; Oceanospirillaceae; Thalassolituus
Subsection I; Family I; Synechococcus
Alphaproteobacteria; SAR11 clade
Oceanospirillales; Oceanospirillaceae
Pseudomonadales; Pseudomonadaceae
Alteromonadales
Cellvibrionales
unassigned Chloroplast
Alphaproteobacteria
Gammaproteobacteria
Bacteroidetes
Proteobacteria
Planctomycetes
Actinobacteria

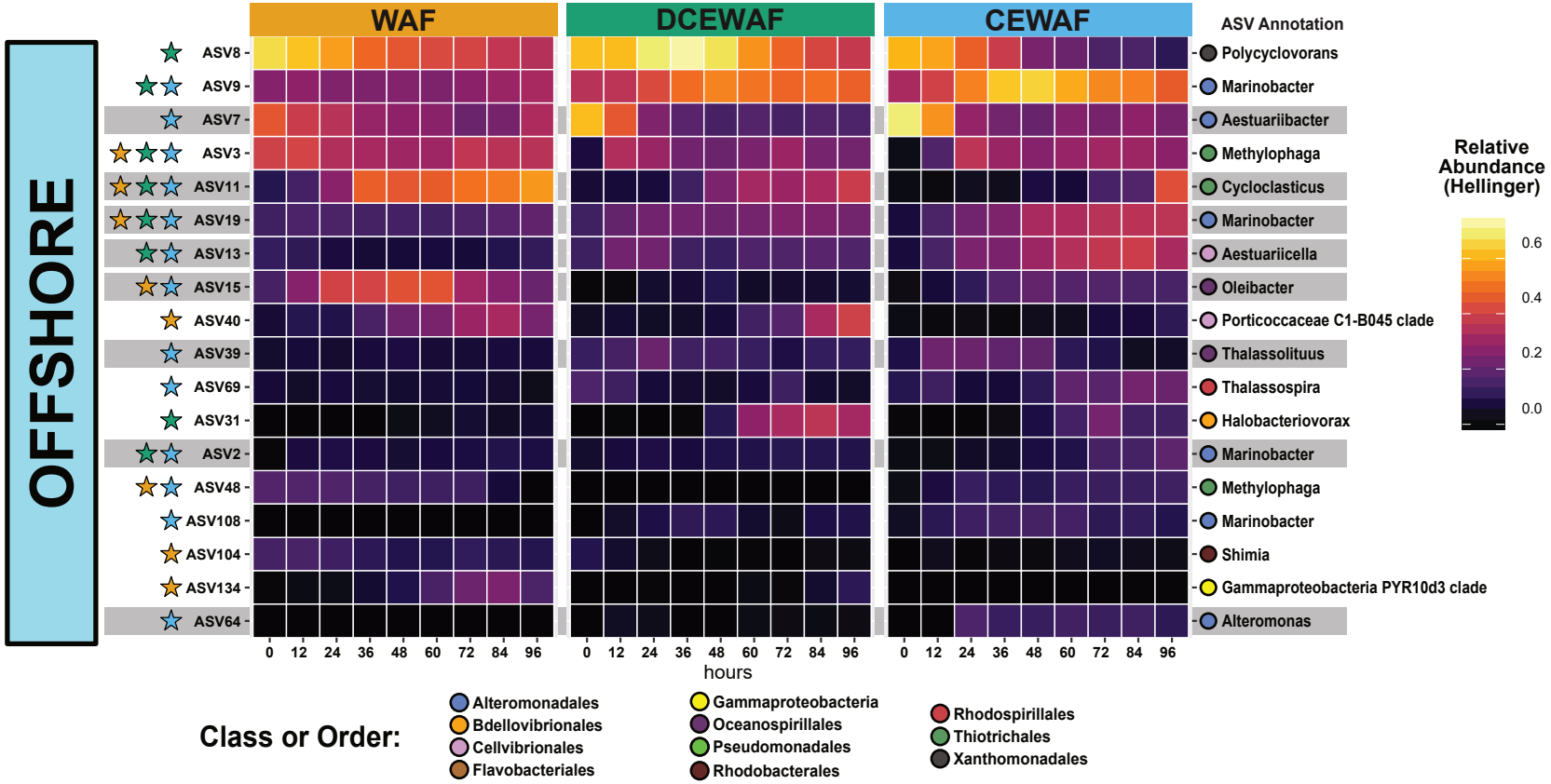
OFFSHORE
WAF
DCEWAF
CEWAF
ASV Annotation
ASV8 - Polycyclovorans
ASV9 - Marinobacter
ASV7 - Aestuariibacter
ASV3 - Methylophaga
ASV11 - Cycloclasticus
ASV19 - Marinobacter
ASV13 - Aestuariicella
ASV15 - Oleibacter
ASV40 - Porticoccaceae C1-B045 clade
ASV39 - Thalassolituus
ASV69 - Thalassospira
ASV31 - Halobacteriovorax
ASV2 - Marinobacter
ASV48 - Methylophaga
ASV108 - Marinobacter
ASV104 - Shimia
ASV134 - Gammaproteobacteria PYR10d3 clade
ASV64 - Alteromonas
0 12 24 36 48 60 72 84 96
hours
Relative Abundance (Hellinger)
0.6
0.4
0.2
0.0
Class or Order:
Alteromonadales
Bdellovibrionales
Cellvibrionales
Flavobacteriales
Gammaproteobacteria
Oceanospirillales
Pseudomonadales
Rhodobacterales
Rhodospirillales
Thiotrichales
Xanthomonadales

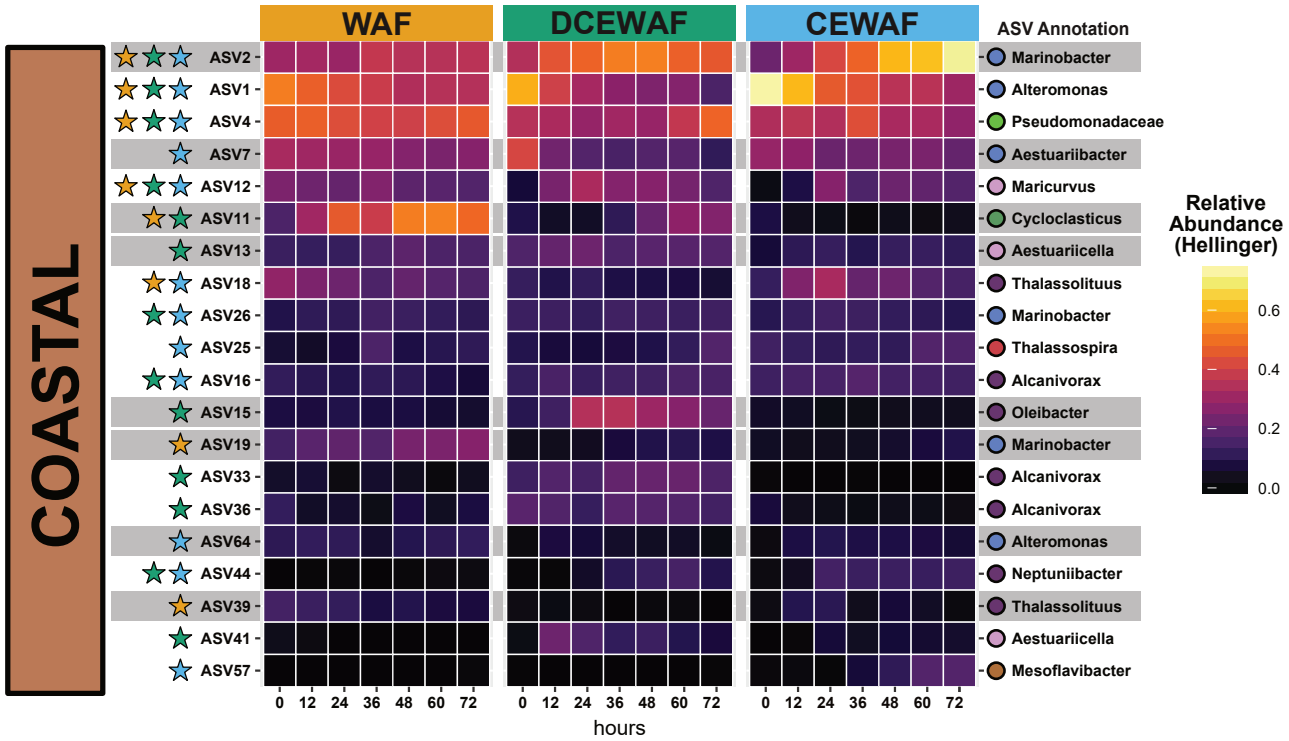
COASTAL
WAF
DCEWAF
CEWAF
ASV Annotation
ASV2 - Marinobacter
ASV1 - Alteromonas
ASV4 - Pseudomonadaceae
ASV7 - Aestuariibacter
ASV12 - Maricurvus
ASV11 - Cycloclasticus
ASV13 - Aestuariicella
ASV18 - Thalassolituus
ASV26 - Marinobacter
ASV25 - Thalassospira
ASV16 - Alcanivorax
ASV15 - Oleibacter
ASV19 - Marinobacter
ASV33 - Alcanivorax
ASV36 - Alcanivorax
ASV64 - Alteromonas
ASV44 - Neptuniibacter
ASV39 - Thalassolituus
ASV41 - Aestuariicella
ASV57 - Mesoflavibacter
0 12 24 36 48 60 72
hours
Relative Abundance (Hellinger)
0.6
0.4
0.2
0.0

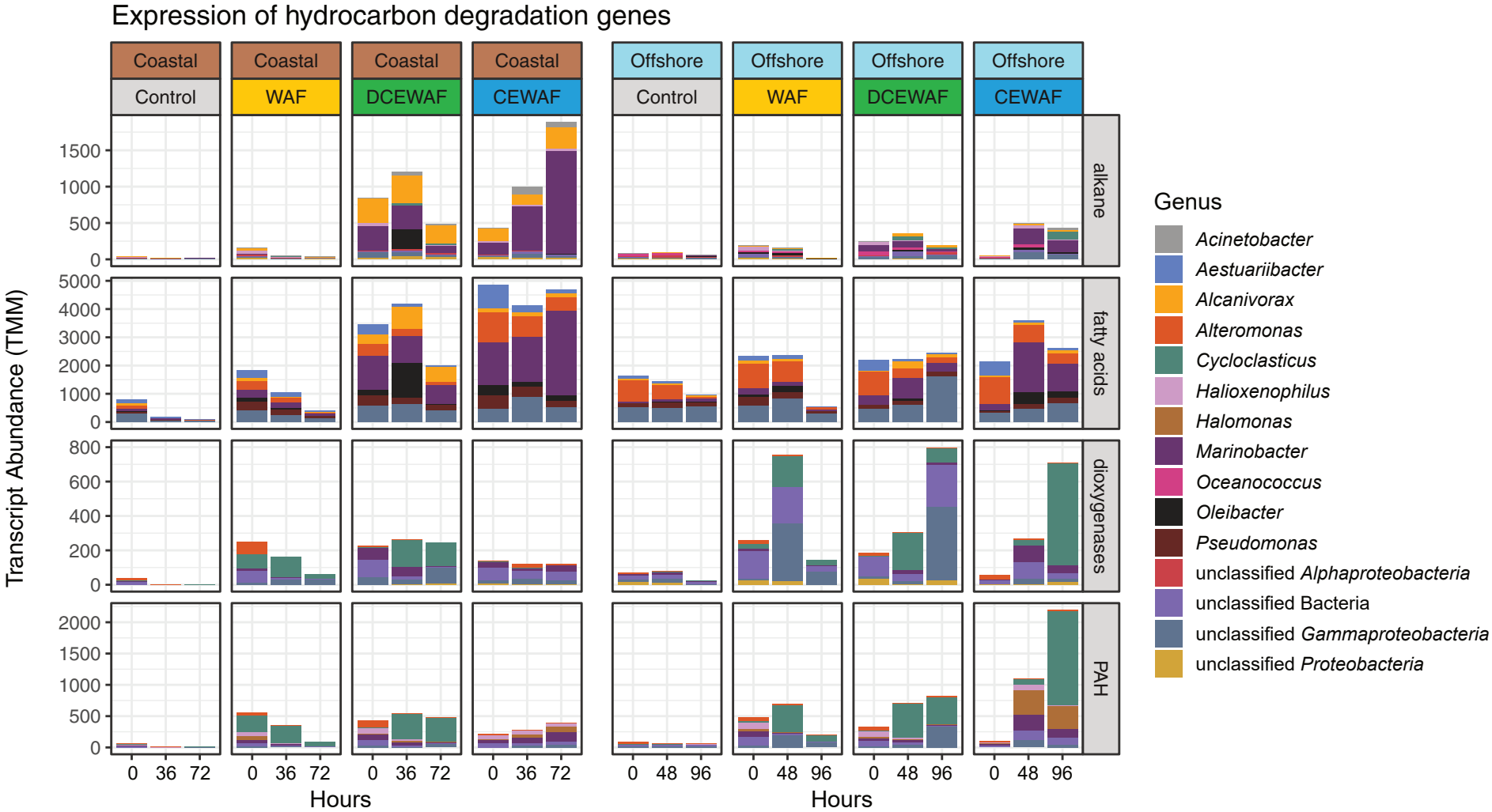
Expression of hydrocarbon degradation genes
Coastal
Control
Coastal
WAF
Coastal
DCEWAF
Coastal
CEWAF
Offshore
Control
Offshore
WAF
Offshore
DCEWAF
Offshore
CEWAF
alkane
fatty acids
dioxygenases
PAH
Transcript Abundance (TMM)
Hours
Hours
Genus
Acinetobacter
Aestuariibacter
Alcanivorax
Alteromonas
Cycloclasticus
Halioxenophilus
Halomonas
Marinobacter
Oceanococcus
Oleibacter
Pseudomonas
unclassified Alphaproteobacteria
unclassified Bacteria
unclassified Gammaproteobacteria
unclassified Proteobacteria

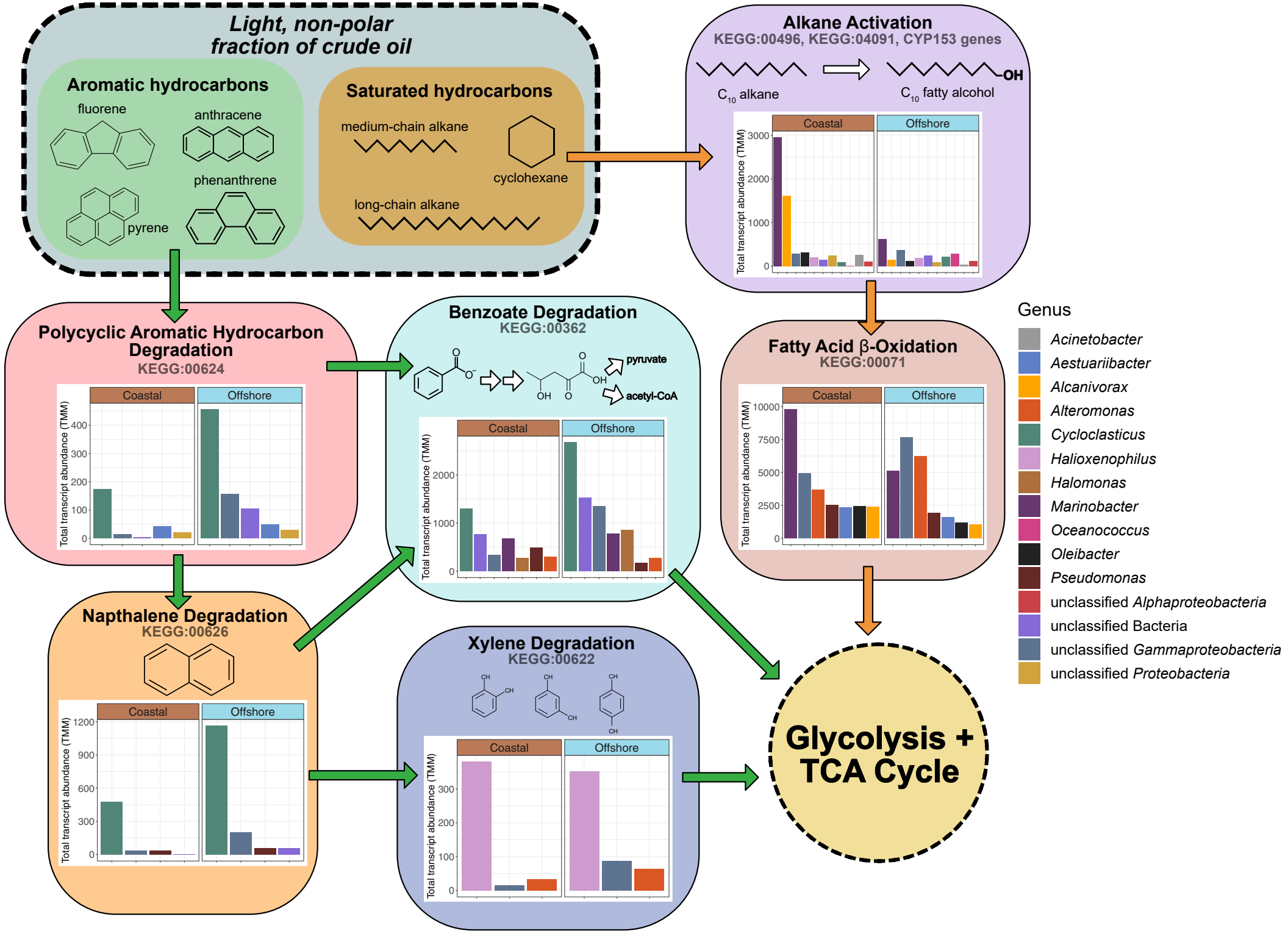
Light, non-polar fraction of crude oil
Aromatic hydrocarbons
fluorene
anthracene
phenanthrene
pyrene
Saturated hydrocarbons
medium-chain alkane
cyclohexane
long-chain alkane
Alkane Activation
KEGG:00496, KEGG:04091, CYP153 genes
C10 alkane
C10 fatty alcohol
OH
Coastal
Offshore
Total transcript abundance (TMM)
Polycyclic Aromatic Hydrocarbon Degradation
KEGG:00624
Benzoate Degradation
KEGG:00362
pyruvate
acetyl-CoA
Fatty Acid β-Oxidation
KEGG:00071
Napthalene Degradation
KEGG:00626
Xylene Degradation
KEGG:00622
Glycolysis + TCA Cycle
Genus
Acinetobacter
Aestuariibacter
Alcanivorax
Alteromonas
Cycloclasticus
Halioxenophilus
Halomonas
Marinobacter
Oceanococcus
Oleibacter
Pseudomonas
unclassified Alphaproteobacteria
unclassified Bacteria
unclassified Gammaproteobacteria
unclassified Proteobacteria

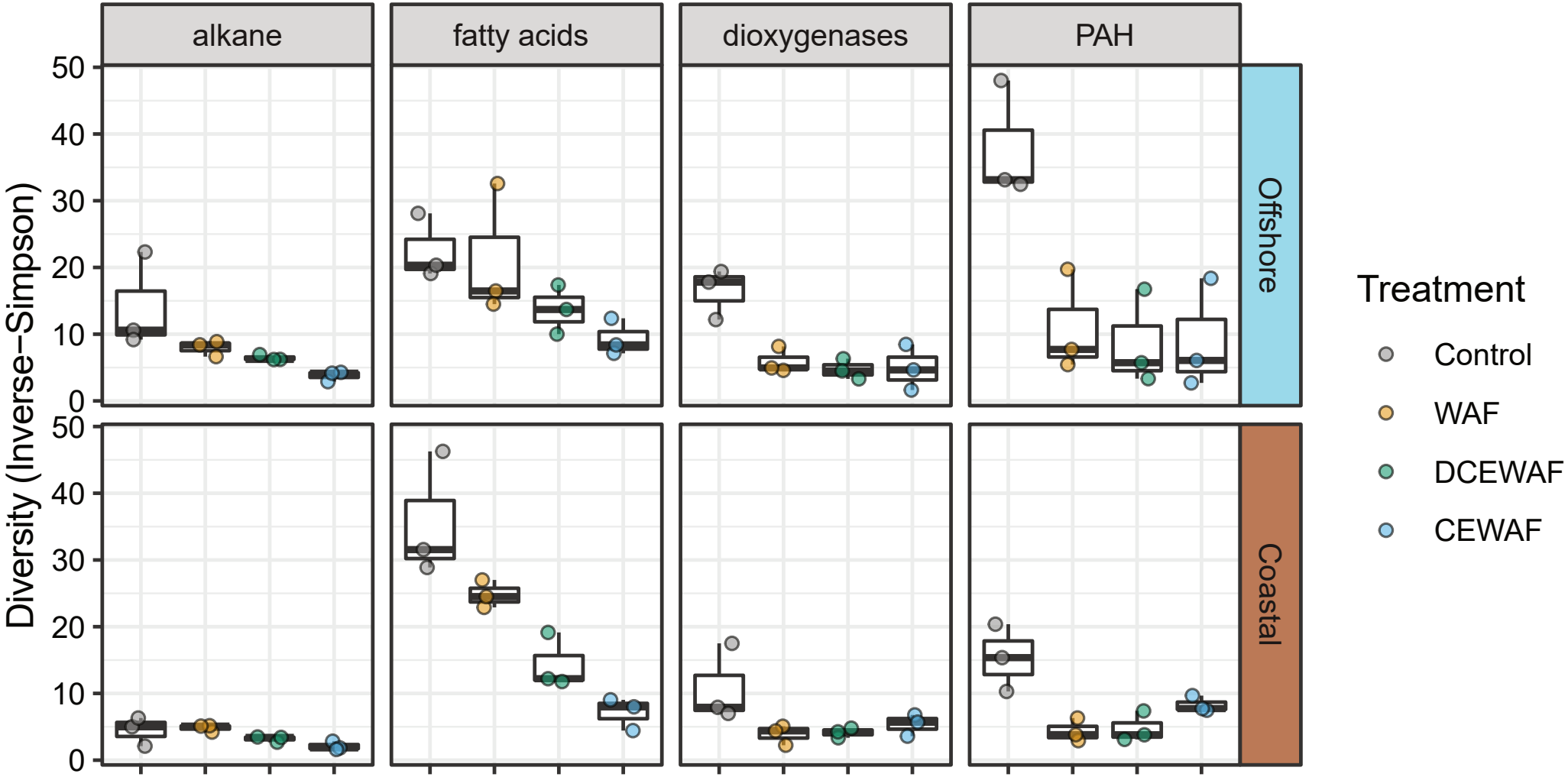
alkane
fatty acids
dioxygenases
PAH
Offshore
Coastal
Diversity (Inverse−Simpson)
0
10
20
30
40
50
Treatment
Control
WAF
DCEWAF
CEWAF